PV Powered Direct Torque Controlled Induction Motor without AC Phase Current Sensors

Muthamizhan.T[1], Ramesh R[2]

Teaching Fellow, Dept. of EEE, CEG, Anna University, Chennai 600025, Tamilnadu, India [1]

Associate Professor, Dept. of EEE, CEG, Anna University, Chennai 600025, Tamilnadu, India[2]

ABSTRACT: The paper presents a low-cost, phase-current reconstruction algorithm for direct torque control three-phase induction motor using the information obtained from only one shunt resistor which is in series with low side switches in a conventional three-phase inverter. The aim is to develop a low-cost high- performance induction motor drive. It uses the dc current to reconstruct the stator currents needed to estimate the motor flux and the electromagnetic torque. Photovoltaic arrays convert solar energy to dc electric power; uses chopper and dc-ac inverter to fed three phase Induction Motor. The chopper used here is current fed full bridge boost dc-dc converter, which is preferred and extensively used in high voltage applications and advantageous over voltage fed converters. The inverter switches are controlled by PWM techniques obtained from SVM-DTC of IM. Simulation results are given to prove the ability of the proposed scheme of reproducing the performances of a SVM- DTC IM drive.

KEYWORDS: Photovoltaic systems, Zero current switching, Induction motors, Space vector pulse width modulation, Direct torque control.

I.INTRODUCTION

The induction motor stands dominant in both industrial and domestic applications.The aim is to develop a low-cost high-performance Space Vector Modulated – Direct Torque Controlled (SVM-DTC) Induction Motor drive as shown in Fig. 1. A low-cost and simple phase-current reconstruction algorithm for three-phase IM under DTC uses dc-link current, dc-link voltage and the voltages applied to the inverters switches of the conventional three-phase inverter. The shunt resistor in series with low side switches are used to draw the dc-link current of a three-phase inverter, the cost of which is less compared to a hall sensor to measure the stator current. The proposed algorithm is robust and very simple and uses the dc-link current to reconstruct the stator currents needed to estimate the motor flux and the electromagnetic torque. The photovoltaic (PV) energy is the most abundant, which is capable of providing the energy needs and having the advantage of photovoltaic pump-storage system. In this system, the use of large banks of batteries is avoided, which are expensive and have one-fifth of the lifetime of a PV panel. The PV characteristics and the issue of maximum power point tracking (MPPT) applied to the induction motor control have been addressed in different ways in the literature [1] - [5]. The fixed frequency phase-shift control enables the implementation of ZCS for all converter switches. Current-fed zero-voltage transition PWM converter use auxiliary network and hence all the power switches are zero-voltage switched or zero-current switched [6], [7]. The space vector pulse width modulation (SVPWM) method and direct torque control techniques for variable frequency drive applications have superior performance characteristics, it has been finding widespread application in recent years [8] - [12]. Sensor less space vector pulse width modulated direct torque controlled induction motor drive utilizing modified stator flux estimation logic has been proposed in literature [13] - [15].

A typical configuration of a batteryless photovoltaic pumping system comprises the following components: photovoltaic panels, MPPT system, current fed full-bridge boost dc-dc converter, dc-ac inverter, three phase induction motor with a closed loop controller. The aim of MPPT is to normalize the real output voltage of PV panel to the voltage at Maximum Power Point. Hence the MPPT adjusts the output power of solar panel. If the PV output voltage is higher than MPP voltage, then transferred power to the load or network is increased, otherwise, it is decreased.Current fed converters are preferred and extensively used in high voltage applications since it is advantageous than the voltage fed

converters. A very high turns–ratio transformer is used to achieve a high output voltage in high voltage applications. The SVM-DTC scheme of an induction motor under varying dynamic conditions, is used to adjust the bandwidth of the torque hysteresis controller to reduce the torque and flux ripples and hence, to improve motor dynamic response.

II.PHOTOVOLTAICS

The conversion of solar energy into electricity using solar cells system is the valuable way of producing the alternative energy. One of the most promising applications of photovoltaic energy is pumping. However, the absence of batteries does not compromise the efficiency of the power conversion chain. Fig. 2 shows the equivalent circuit of the solar cell.The V-I characteristic of a single-junction P-N under illumination can be written as follows:

$$I = I_L - I_0\left[\exp\left(\frac{q(V + IR_S)}{nkT}\right) - 1\right] \qquad (1)$$

Where the net current is the difference of photocurrent and diode current, V is the voltage, T is the absolute temperature and R_S is the series resistance inside each cell in connection between the cells. The shunt resistance R_{sh} is neglected. A single shunt diode was used with the diode quality factor set to achieve the best curve match.
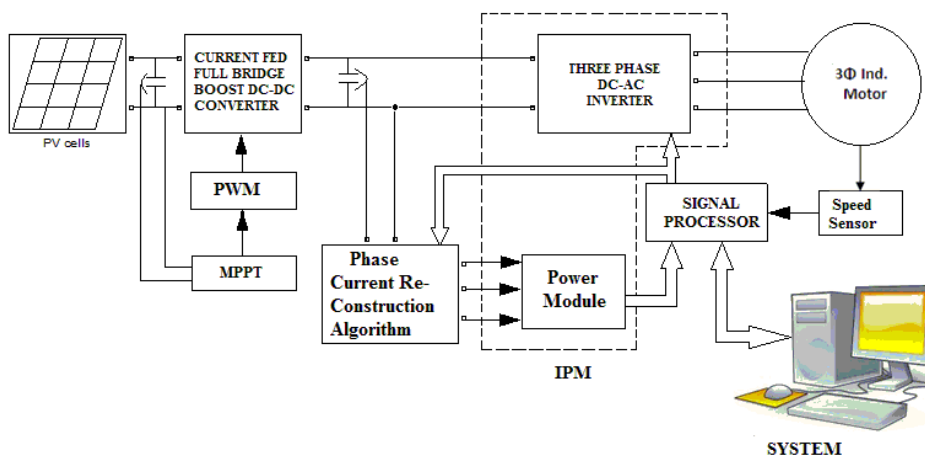

Fig. 1 Block diagram of induction motor with phase current re-construction algorithm

Solar cells are usually connected in series, in the modules, creating an additive voltage and in parallel to yield higher amperage. Modules are then interconnected, in series and parallel to create the desired peak dc voltage and current.
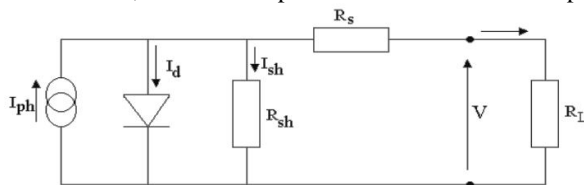

Fig. 2 Equivalent circuit of the solar cell

The "Hill Climbing" MPPT algorithm perturbs the voltage in one direction and evaluates the corresponding difference (sign) of the power. If the power is increasing, the algorithm will move the voltage in the same direction; otherwise, it will reverse the direction. The "Hill Climbing" algorithm can be confused, and track the MPP in the wrong direction, in case of rapidly changing atmospheric conditions, when the change in PV power caused by change in irradiance is larger than the change in PV power as a function of the perturbation. The "Hill Climbing" will not be confused, if and only if

$$|\Delta P_u| > |\Delta P_g| \qquad (2)$$

where ΔP_u is the change in power as function of change in voltage, and ΔP_g is the change in power as function of change in irradiance. The hill climbing MPPT is optimized in respect with the sampling interval (Ta) and minimum step size (ΔV_d) in order to follow a certain irradiance ramp (dg/dt). The approach is based on a second-order Taylor approximation of the PV model including resistive parts. Fig. 3 shows the V-I characteristics of the 1 kW solar array and Fig. 4 shows the P-V characteristics of the 1 kW solar array. If operating point of load is on the left of MPP, in other words if the module works as a current source, the error signal can be written as

$$\frac{\partial P_{module}}{\partial V_{module}} < 0 \Rightarrow M = M - \Delta M \tag{3}$$

In the opposite case, PV module acts as a voltage source, and error signal (M) is calculated as

$$\frac{\partial P_{module}}{\partial V_{module}} > 0 \Rightarrow M = M + \Delta M \tag{4}$$

At Maximum power point, error will be zero and expression is written as follows:

$$\frac{\partial P_{module}}{\partial V_{module}} = 0 \Rightarrow M = M \, or \, \Delta M = 0 \tag{5}$$

It is proved that the "Hill Climbing" algorithm is the one of the best method to extract the maximum power and hence this paper uses hill climbing algorithm to extract the maximum power.
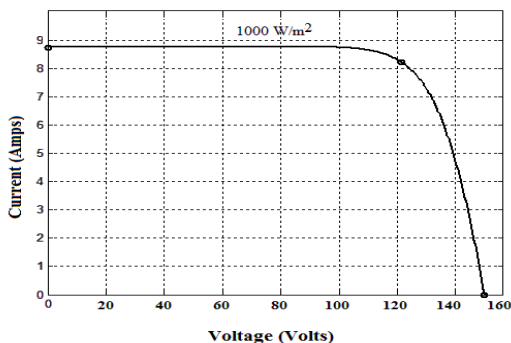

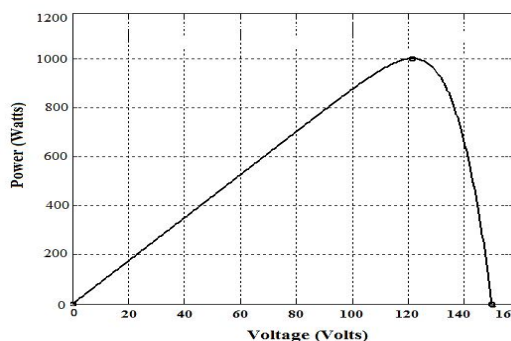Fig. 3 V-I Characteristics of 1KW solar array

Fig. 4 P - V Characteristics of 1KW solar array

III.CURRENT FED FULL-BRIDGE BOOST DC-DC CONVERTER

Current fed converters shown in Fig.5, are preferred and extensively used in high voltage applications since it is advantageous than the voltage fed converters. A very high turns–ratio transformer is used to achieve a high output voltage in high voltage applications. The disadvantage of using large turns ratio transformer is the parasitic components (parasitic capacitance and leakage inductance) generate high voltage and current spikes, results in switching losses in the power devices, which has been overcome by Zero Current Switching (ZCS) operation. Constant on-time control methodology is utilized to achieve ZCS and a variable frequency control scheme is used to regulate the output voltage.In order to decrease the volume and weight of the dc-dc converter, higher switching frequency is chosen. Increasing switching frequency leads to increased switching losses which in turns reduces converters efficiency. Soft switching techniques are used in PWM dc-dc converters to reduce switching losses and Electro Magnetic Interference (EMI). Soft-switching of the dc-dc converter have either turn-on or turn-off switching losses in a power switches are eliminated. Soft switching in current fed full-bridge boost dc-dc converter has been achieved by Zero current Switching (ZCS)technique in high frequency applications using IGBT switches in the dc-dc converter.
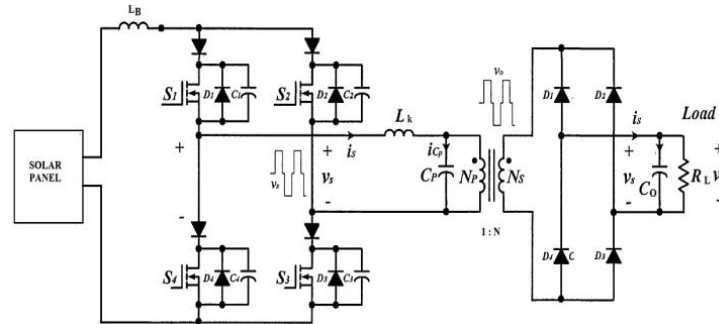
Fig. 5 Current fed full-bridge boost dc-dc converter.

The dc-dc converter utilizes the leakage inductance and the parasitic capacitance of the high-voltage transformer in order to achieve the ZCS operation. The switch can be implemented by an IGBT in series with a reverse blocking diode, an IGBT with reverse–voltage blocking capability. The current and voltage during the turning on and off of the switch is shown in Fig. 6 and the power loss of the switching component is 0.3W to 1W by ZCS.The current fed full bridge boost dc-dc converter yields an output voltage of 600 V while the solar panel input voltage is (120-180)V, the current is continuous and the converter driven near resonance.The switching pattern applied to the switches of the full bridge, utilizing the leakage inductance and the parasitic capacitance of the high-frequency transformer to achieve the ZCS operation across the switches. Fig. 7 shows the voltages at the input and output side of the high frequency transformer of turns ratio 1:4.The transformer output is connected to the diode bridge rectifier and the ripple is filtered with a bulk capacitor of value 2200 μF. The output voltage, current and power of the dc-dc converter is plotted in the Fig. 8.
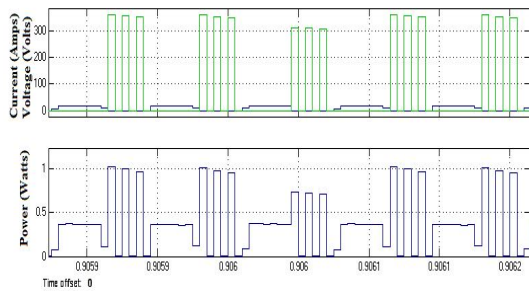

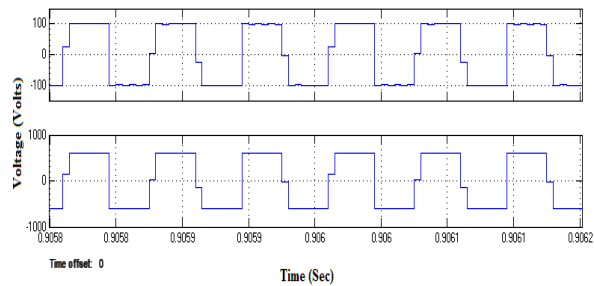Fig. 6 Current, voltage and power loss across the switch during ZCS of the dc-dc converter

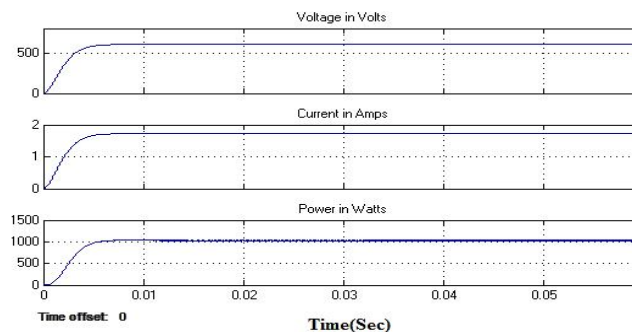Fig. 7 Transformer input and output voltage of the dc-dc converter

Fig. 8 Output voltage, current and power waveform of the dc-dc converter

IV.SVM - DTC OF INDUCTION MOTOR

The phase currents are estimated by the dc-link current measurement processes. The phase voltages and currents required in the classical direct torque controller is reconstructed using the dc-link voltage and dc-link current, instead of the stator phase voltages sensed from induction motor using hall sensors.The stator flux vector and the electromagnetic torque are directly calculated from the voltage and the current derived from a single dc-link voltage sensor from a voltage divider network and a single dc-link current sensor by using a shunt resistor.This algorithm does not require additional computation burden or other motor parameter knowledge. The simulation of the low cost direct torque controlled induction motor is done using MATLAB/SIMULINK simulation software. The solar panel output is fed to current fed full bridge boost dc-dc converter. The dc output voltage is filtered with a bulk capacitor and the dc voltage is given as input to the three phase inverter connected to the three phase induction motor. Here PI controller is used to tune the speed error which is used to generate the torque reference signal.

Classical controllers with limitations have been used to control induction machines in achieving desired dynamic response. One modification of the basic DTC is used for estimating the three-phase currents from a single dc-link current sensor. On the modification, the need of an additional current sensor requirement is minimized. The six voltage vector is applied at each cycle period, for prefixed time intervals for the Space Vector Modulation (SVM) technique.

TABLE I
DTC SWITCHING TABLE

Sector		1	2	3	4	5	6
$C_\emptyset = -1$	$c_t = -1$	V_2	V_3	V_4	V_5	V_6	V_1
	$c_t = 0$	V_7	V_0	V_7	V_0	V_7	V_0
	$c_t = +1$	V_6	V_1	V_2	V_3	V_4	V_5
$C_\emptyset = +1$	$c_t = -1$	V_3	V_4	V_5	V_6	V_1	V_2
	$c_t = 0$	V_0	V_7	V_0	V_7	V_0	V_7
	$c_t = +1$	V_5	V_6	V_1	V_2	V_3	V_4

By using this modulation strategy, the voltage vectors are synthesized with respect to those used in the basic DTC technique from −30∘ to 30∘. The DTC switching table is tabulated in Table I. The PWMgenerated by the space vector pulse width modulation techniques for the classical DTC is as shown in the Fig. 9. The output voltage for various switching patterns can be obtained by considering an example of Space voltage V_6 (state 101); the output voltages V_{an}, V_{bn} and V_{cn} are obtained by the equivalent circuit as shown in Fig. 10.The phase voltages and currents are reconstructed using the dc-link voltage, dc-link current and the voltages applied to the switches. The phase voltages and phase currents of the stator of three phase inductor motor are reconstructed and the simulated waveforms are given in the Fig.11.
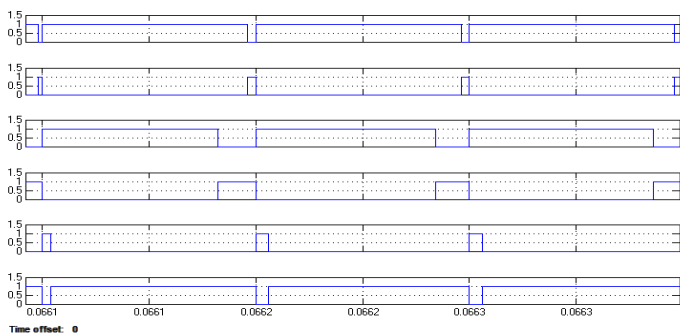

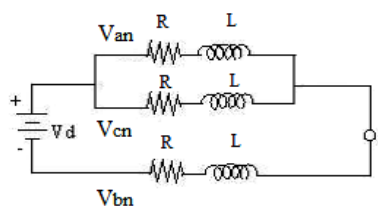Fig. 9 Pulse generated in the SVPWM-Classical DTC IM

Fig. 10 Equivalent circuit to find V_{an}, V_{bn} and V_{cn}

TABLE II
SUMMARY OF INVERTER SWITCHING STATES

Name	C	B	A	V_{an}	V_{bn}	V_{cn}
V_0	0	0	0	0	0	0
V_1	0	0	1	$2V_{dc}/3$	$-V_{dc}/3$	$-V_{dc}/3$
V_2	0	1	0	$V_{dc}/3$	$V_{dc}/3$	$-2V_{dc}/3$
V_3	0	1	1	$-V_{dc}/3$	$2V_{dc}/3$	$-V_{dc}/3$
V_4	1	0	0	$-2V_{dc}/3$	$V_{dc}/3$	$V_{dc}/3$
V_5	1	0	1	$-V_{dc}/3$	$-V_{dc}/3$	$2V_{dc}/3$
V_6	1	1	0	$V_{dc}/3$	$-2V_{dc}/3$	$V_{dc}/3$
V_7	1	1	1	0	0	0

The output voltages V_{an}, V_{bn} and V_{cn} can be calculated using the Equation 3.18 and are given as follows:

$$Z_{eq} = \frac{3Z}{2} \tag{6}$$

$$V_{an} = V_{cn} = V_{dc}\left.\frac{z}{2}\right/3\frac{z}{2} = \frac{V_{dc}}{3} \tag{7}$$

$$V_{bn} = -V_{dc}.z\left/3\frac{z}{2}\right. = \frac{-2V_{dc}}{3} \tag{8}$$

where V_{dc} is the dc link voltage. Similarly we can calculate the values of V_{an}, V_{bn} and V_{cn} for the other five nonzero states. V_0 and V_1 are the zero states of the space voltage. The inverter switching states is tabulated in Table II and the parameters of the induction motor are tabulated in Table III.
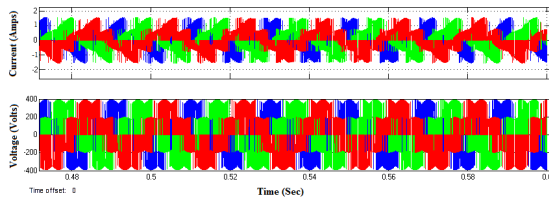

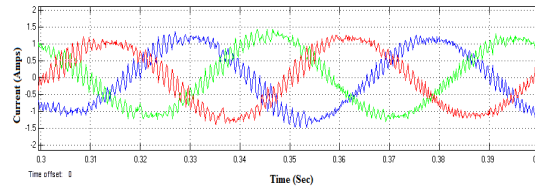Fig. 11 Calculated phase current and phase voltage waveforms

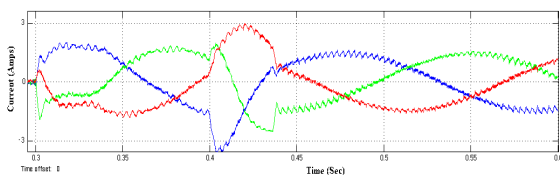Fig. 12 Stator currents vs time characteristics of classical DTC IM

Fig. 13 Rotor currents vs time characteristics of classical DTC IM

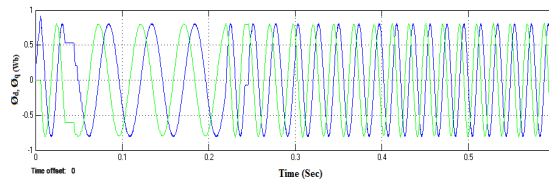Fig. 14 $\emptyset_d$, $\emptyset_q$ vs time characteristics of classical DTC IM
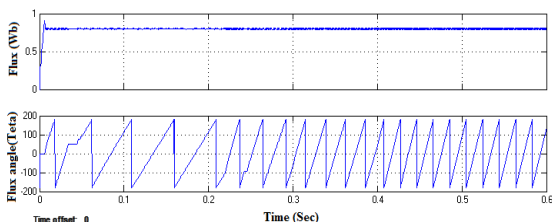

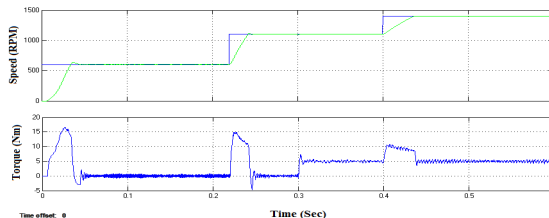Fig. 15 Flux, flux angle vs time characteristics of classical DTC IM

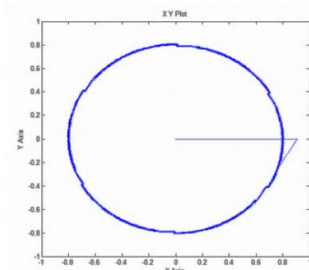Fig. 16 Speed and torque response curve of classical DTC IM

Fig. 17 Stator flux locus using classical DTC

Fig.12 and Fig.13 shows the stator and rotor current measured in the classical direct torque controlled induction motor respectively using MATLAB/SIMULINK software.Fig. 14 measures the direct and quadrature axis component of the flux, $\emptyset_d$ and $\emptyset_q$, and Fig. 17 shows the Stator flux locus of the space vector modulated classical DTC IM.Fig. 15 shows the measured total flux $\emptyset$, flux angle θ and Fig. 16 shows the speed characteristics of the classical DTC IM using SVM

TABLE III
PARAMETERS OF THE INDUCTION MOTOR

Parameters	Ratings
Rated power	1 HP
Rated voltage	415V
Rated speed	1440 RPM
Pole pairs	2
Stator resistance	8.35 Ω
Rotor resistance	8.43 Ω
Stator leakage inductance	32 mH
Rotor leakage inductance	32 mH
Air gap inductance	0.601 H
Rotor time constant (J)	0.0051Kg.m^2
Friction factor(F)	0.06 Nm.s

The speed of the induction motor is set at 600 RPM, 1100RPM and 1400 RPM respectively at 0s, 0.22s and 0.4s. At 600 RPM, the motor speed reaches in 0.065s but settles down 600 RPM at 0.075s. At 0.22s when the reference speed is set to 1100 RPM the motor speed starts to follows the speed from 1100 RPM in 0.026s with a little overshoot. At 0.4s the speed is set to 1400RPM and the motor speed follows reach the set speed at 0.465s.Fig. 16 also shows the electromagnetic torque Vs time curve, where the torque settles down at 5 Nm finally with a ripple of 2 Nm but the transient response of the electromagnetic torque curve has more ripple. Direct torque control technique are used by many researchers because of it finds extensive applications with various ac machine types such as induction motor, PMSM, PM Brushless, and Reluctance motor.

V. CONCLUSION

A low-cost, phase-current reconstruction algorithm for a PV powered space vector modulated- direct torque controlled three-phase induction motor was proposed in this paper. The number of sensor in the induction motor drive is reduced by using phase-current reconstruction algorithm. The maximum dc power can be obtained from the PV array by utilizing the "HILL CLIMBING" algorithm. The advantage of using current fed full bridge boost dc-dc converter here is that all of the parasitic capacitances and inductances are included in the resonant or filter circuits and the system does not generate parasitic oscillations and the output is without any uncontrolled high voltage and current spikes.The conclusion is that the whole performance of the system is improved compared to a vector control of induction motor. The settling time of the speed and ripples present in the torque are reduced hence DTC method are preferred than vector control

REFERENCES

[1]   S.B. Kjaer, "Evaluation of the "Hill Climbing" and the "Incremental Conductance", Maximum Power Point Trackers for Photovoltaic Power System", IEEE Transactions on Energy Conversion, vol. 27, no. 4, pp. 922-929' 2012.
[2]   T. Esram and P. L. Chapman, "Comparison of Photovoltaic Array Maximum Power Point Tracking Technique", IEEE Transactions on Energy Conversion, vol. 22, no. 2, pp. 439-449, 2007.
[3]   M.A. Vitorino, M.B. de Rossiter Correa, C.B. Jacobina and A.M.N. Lima, "An Effective Induction Motor Control for Photovoltaic Pumping", IEEE Transactions on Industrial Electronics, vol. 58, no. 4, pp. 1162-1170, 2011.
[4]   T. Muthamizhan & R. Ramesh, "Design and Simulation of PV driven three phase Induction motor", International Review on Modelling and Simulations, vol. 6, no. 2, pp. 412-418, April. 2013.
[5]   Y. Yao, P. Bustamante R.S. Ramshaw, "Improvement Of Induction Motor Drive Systems Supplied By Photovoltaic Arrays With Frequency Control", IEEE Transactions on Energy Conversion, vol. 9, no. 2, pp. 256-262,1994.
[6]   R.Y. Chen, T.J. Liang, J.F.Chen, R.L. Lin and K.C. Tseng, 'Study and implementation of a current-fed full-bridge boost DC–DC converter with zero-current switching for high-voltage applications', IEEE Transactions on Industry Applications, vol. 44, no. 4, pp. 1218-1226, 2008.
[7]   L. Zhou and X. Ruan, "A zero-current and zero-voltage-switching PWM boost full-bridge converter', Proceedings of thirty-fourth annual conference in Power Electronics Specialist Conference, 2003, vol. 2, pp. 957-962.
[8]   B. Singh, S. Jain and S. Dwivedi, "Direct Torque Control Induction Motor Drive with Improved Flux Response" Advances in Power Electronics, vol. 2012, pp. 1-11, 2012.
[9]   E.E. El-kholy, R. Kennel, A. El-refaei, S.A. El-Latif and F. Elkady, "Robust Space–Vector Current Control for Induction Motor Drives', Journal of Electrical Engineering, vol. 57, no. 2, pp. 61–68, 2006.
[10] K. Zhou and D. Wang, "Relationship Between Space-Vector Modulation and Three-Phase Carrier-Based PWM: A Comprehensive Analysis', IEEE Transactions on Industrial Electronics, vol. 49, no. 1, pp. 186-196, 2002.
[11] G.S. Buja and M.P. Kazmierkowski, 'Direct torque control of PWM inverter-fed AC motors - A survey", IEEE Transactions on Industrial Electronics, vol. 51, no. 4, pp. 744-757, 2004.
[12] S. R. Maturu and A. Vujji, "SVPWM Based Speed Control of Induction Motor Drive with Using V/F Control Based 3-Level Inverter", VSRD International Journal of Electrical, Electronics & Communication Engineering, vol. 2, no. 7, pp. 421-437, 2012.
[13] A. Sivakumar, T. Muthamizhan, N. O. Gunasekhar & R. Ramesh, "A Novel Sensorless Speed Control Strategy of Induction Motor Based on Vector Control", International Review of Electrical Engineering, vol. 8, no. 4, pp. 1211-1217, Aug. 2013.
[14] A. Choudhury and K. Chatterjee, 'Speed sensor less direct torque controlled induction motor drive with constant switching frequency operation', Proceedings of the international conference on Energytech,2011, pp. 1-6.
[15] K.K. Yoon and S.H. Kim, "Sensorless Speed Control of Induction Motor by Direct Torque Control with Numerical Model", Journal of theKorean Society of Marine Engineering, vol. 36, no. 6, pp. 830-836, 2012.